SLAC-PUB-3131
June 1983
(I)

SEARCH FOR THE BEST TIMING STRATEGY IN HIGH PRECISION DRIFT CHAMBERS*

J. VA'VRA
Stanford Linear Accelerator Center
Stanford University, Stanford, California 94305

ABSTRACT

Computer simulated drift chamber pulses are used to investigate various possible timing strategies in the drift chambers. In particular, the leading edge, the multiple threshold and the flash ADC timing methods are compared. Although the presented method is general for any drift geometry, we concentrate our discussion on the jet chambers where the drift velocity is about 3-5 cm/μsec and the individual ionization clusters are not resolved due to a finite speed of our electronics. We will not discuss the geometries where the drift time is expanded further and the individual clusters can be recorded (this is covered by a talk by A. H. Walenta).

Presented at the 2nd Pisa Meeting on Advanced Detectors,
Castiglione della Pescaia, Italy, June 3-7, 1983.

---

* Work supported by the Department of Energy, contract DE-AC03-76SF00515.

INTRODUCTION

The Monte Carlo method presented in this paper is a result of a lengthly effort. The initial motivation was to understand the drift time distribution in the jet chambers for various track angles in large magnetic fields,[1]-[2] double track separation in a specific design of the SLC detector[3] and the effect of focusing electrode structures on the width of electron drift time distribution (unpublished).

In this paper we present results of the resolution study. We try to investigate the tracking resolution dependence on variables such as the gas pressure; the amplifier response; the gain in the chamber; the detection method such as the single, double, multiple thresholds or the flash ADC; the geometry of the charge collection; whether we run the drift cell correctly both from point of view of the resolution and the long pulse tails, etc.

The problem of prediction of the chamber resolution is quite complex since there is a large number of parameters to consider. One cannot avoid to neglect some of them, simply to manage the overall complexity. Our aim is to address the limits of the resolution primarily due to the physics of the detection process. Clearly, once a given detection technique is chosen, one can then include the intricate details of functioning of a particular circuit, specific details of signal propagation along resistive wires, as well as a list of other typical systematic contributions to the overall resolution.

Why the Monte Carlo as opposed to analytical calculations?[4] Although the hand calculation has a great advantage because it can be done quickly, it cannot possibly go to such a detail and insight as one can do in the Monte Carlo approach. Remember, in our approach we are not limited to a particular drift geometry or a particular method of detection of the drifting charge.

PRINCIPLE OF THE METHOD

The first step is to simulate the drift pulses by convoluting three basic broadening contributions (see Appendix A for more details):

1. Drift distributions of the arrival of individual electrons at the anode wire using a correct two-dimensional electrostatic field.
2. Response of the avalanche due to the motion of positive ions including its fluctuations.
3. Finally, we measure the response of the amplifier to an impulse charge and convolute it with all other contributions.

Once the waveform is generated, we define a threshold as, say $\sim 5-10\%$ of the average peak value and then find the crossing point of the waveform at the threshold. In this way, we can determine the expected resolution for a given timing strategy, such as the leading edge

timing with a single threshold, multiple threshold, centroid timing using a waveform digitizer such as the flash ADC, et cetera.

The pulse waveforms are difficult to check using the real particles because even the 10 ns digitizer does not reveal a full detail of the pulse shape. We have used the nitrogen laser[5] to compare the laser drift pulses and the program simulation. Since the laser produces a continuous ionization, the drift pulses are very smooth and the average is easy to determine by polaroid pictures. The clustering was switched off in the program for this comparison. The experimental results agree very well with the program's prediction.

Finally, the very important point to stress is that our method assumes a full linearity in the process of the waveform formation, i.e. all drifting electrons have equal weight. This can be satisfied only at low gains. At higher gains on the wire the later arriving charge will be screened by the previously occuring avalanches and its weight is lowered. Therefore, for instance we expect that the centroid flash ADC timing at high gains will provide results similar to the leading edge timing, although at low gains both methods lead to significantly different results.

EXAMPLE OF THE RESOLUTION STUDY IN A LARGE JET CHAMBER

The nature of the problem is such that only few generalities can be made and that one has to deal with specific examples. In this chapter we consider the examples of the jet chambers, where anode wires are separated by the potential wires with 4-5 mm neighbour to neighbour wire spacing. Such a spacing will allow to use 20-50 μm diameter anode wires, and therefore enable longer chamber designs. Practical examples of such designs are JADE,[6] AFS[7] and OPAL[8] drift chambers.

A common feature of all these designs is the fact that the drift time of each electron depends on its origin along the track sample. An illustration of this feature is shown in Fig. 1. The "U-shape" geometrical effect together with a finite ionization and clustering of the electron distribution within the sample is causing the randomness in the drift time distribution, which is a projection of the "U-shape" distribution on the drift time axis of the same graph. Unfortunately, there is a little one can do to flatten the "U-shape" distribution in this particular drift structure, since the only variable one has is the voltage on the potential wire. When the potential wires collect fully the charge, one has the least amount of the electrons contributing to the first arriving charge, and if they do not collect the charge, as is required in the dE/dx measuring chamber, one makes the "U-shape" distribution shallower and as a consequence one improves the timing resolution using for instance the leading edge timing.

Figure 2 shows an example of the pulse shapes as they would appear if we use 100 MHz digitizer. The simulation assumes an amplifier with 10 ns rise time and 50 ns fall time response

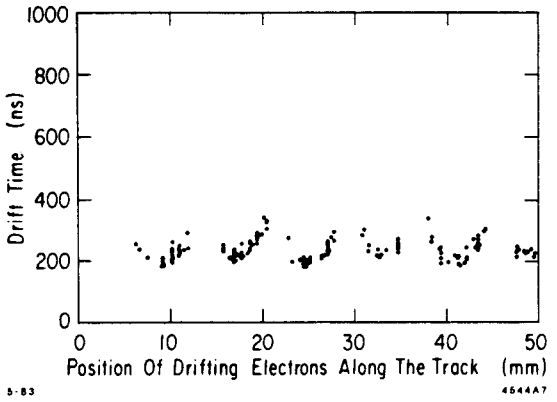

Fig. 1. The "U-shape" distributions in the SLD cell[3] with 90% Ar + 10% C_4H_{10} at 1 atm, B = 10 kG, 4 mm wire-wire distance and .5 mm impact parameter of the track and the wire plane.

to a step charge and the use of the zero-pole filter to suppress the 1/t tail due to positive ions.[9] However, even the 100 MHz digitizer will not reveal the full detail of the pulse waveform as can be seen in Fig. 3, where we assume a hypothetical 1 ns digitizer. We define the thresholds T1-T4 at 5, 10, 15 and 20% of the average peak value and find the corresponding crossing points of the pulse and each threshold. If we loop over say $\sim$ 100 events, we can build up the histograms of the resolution for various timing strategies. Example of such distributions can be seen in Figs. 4 and 5, which are generated for 1 and 4 atm pressure operations respectively and with the identical pulse shaping conditions as in Fig. 3. Clearly, the case (a) of Figs. 4 and 5 is not realizable in practice, however, it serves as a useful reference for our discussion. One can see that at 1 atm of pressure one can improve the first electron timing resolution if we average over the electron time arrivals in the first 10-15 ns. At 4 atm one would have to average over even smaller time interval of less than 5 ns. As we increase the time interval over which we are averaging, the resulting resolution gets worse. This can be explained by a combination of the previously mentioned "U-shape" geometrical effects plus the finite clustering ionization statistics. By making a cut on the electron arrival time we make a cut on the geometrical acceptance (making the "U-shape" artificially flatter). That makes the drift time distribution less sensitive to the fluctuations in the ionization. One can say that in the limit of infinitely fast electronics capable of digitizing the time of arrival of every arriving electron, one can achieve the $1/\sqrt{N}$ improvement factor in the center of gravity timing compared to the first electron timing, where N is a number of electrons contributing to a particular timing cut. However, as soon as we remove the assumption of the infinitely fast electronics, we cannot realize this improvement factor, because we lose the full information about the sample (the only way to recover the full knowledge about the event practically, is to go to the time expansion concept,[10] which brings, of course, other complications). The cases (b) and (c) in Figs. 4 and 5 show the resolution results with the realistic pulse shapes.

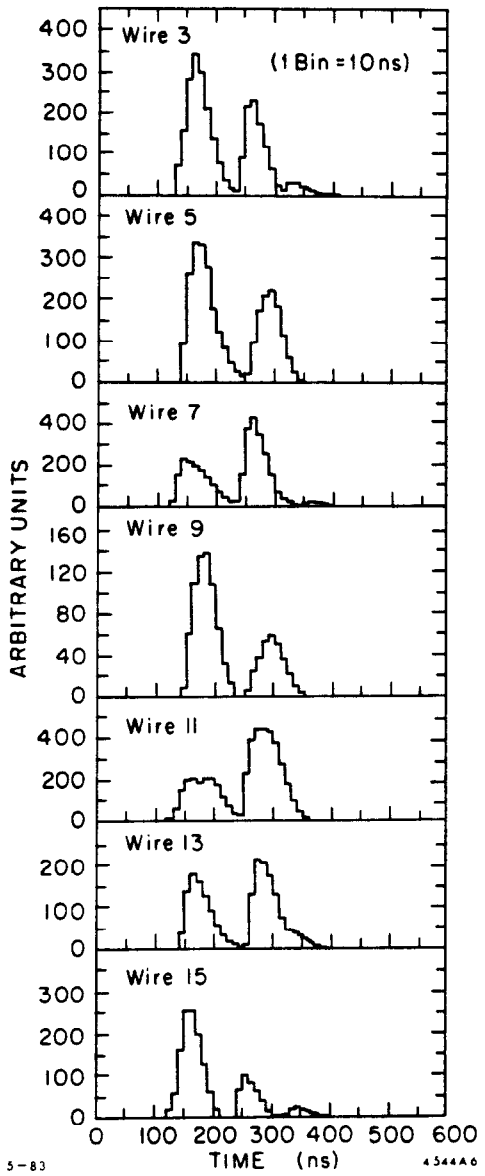

Fig. 2. The drift pulses in the same cell as in Fig. 1 as they would be seen by a 100 MHz digitizer. Simulation is for 90% Ar + 9% CO_2 + 1% CH_4 at 1 atm, B = 5 kG, 5 mm double track separation.

One can see that at best we can achieve the quality of the first electron timing. This applies both for a simple single threshold timing as well as for more complicated double or multiple threshold timing. One should say that the multiple threshold timing would be equivalent to a hypothetical 1-2 ns digitizer! We also should stress that we have used exactly the same events in all plots of Figs. 4 and 5, i.e. we do not apply any quality cut on the pulse waveforms (see discussion about this point later). On the basis of what we have said so far there would not be much motivation to instrument the double threshold electronics. However, one can see that the double threshold timing can approach the first electron timing even with higher thresholds. We interpret this as an indication that we can lower the gain in the chamber and still achieve

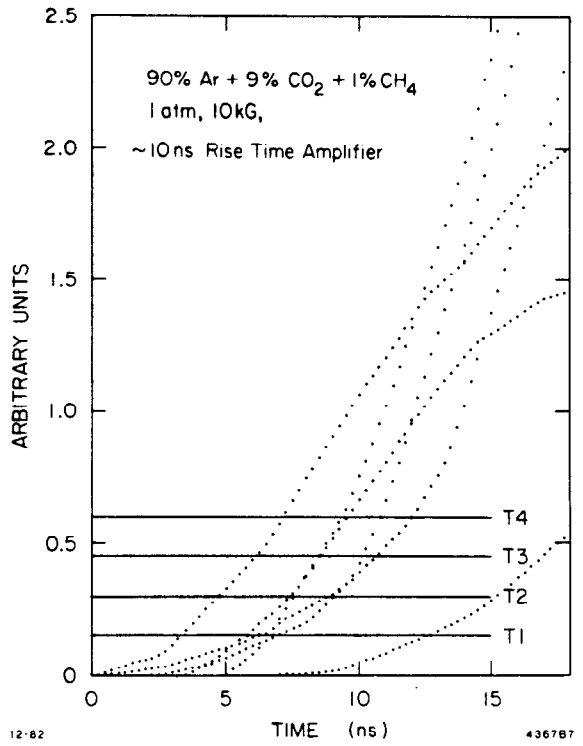

Fig. 3. Details of the drift pulses as they would be seen by a hypothetical 1 ns digitizer. The conditions are the same as in Fig. 2, except B = 10 kG. T1-T4 threshold corresponds to 5, 10, 15 and 20% of the average peak.

the first electron timing quality. Lowering the gain in the chamber might be significant from the life time point of view.

Let's now discuss the timing quality we might achieve with the flash ADC schemes, which are waveform digitizers operating with up to 10 ns sampling frequency, i.e. considerably less often than with the multiple threshold scheme. This method was pioneered experimentally by the JADE group.[8] Figure 6 indicates the method used in our study. First, we create a reference pulse by averaging over a number of pulse shapes, which are normalized to their peak values. We then move the reference pulse through the particular FADC pulse, which is known every 10 ns. We then take a certain number of the FADC points and the corresponding reference points and calculate a quantity $Q \sim \chi^2$. The timing point for a particular event is taken as a minimum of the Q-curve. Figure 7 shows the results of the resolution study with the FADC's at 4 atm. We should say that the events are identical to those of Fig. 5 without any quality cut on the pulse shapes. We can see that a parabola fit to 8 points [Fig. 7(a)] gives worse timing compared to weighted 3-point method [Fig. 7(f)], where the very first FADC point is weighted the most. However, Fig. 8(c) indicates that for large drift cells like JADE or OPAL, a simple parabola fit with 5-8 points gives better overall timing resolution throughout the cell. This is simply because the weighted algorithm weights more the first arriving electrons and therefore we are more sensitive to diffusion. However, in small drift

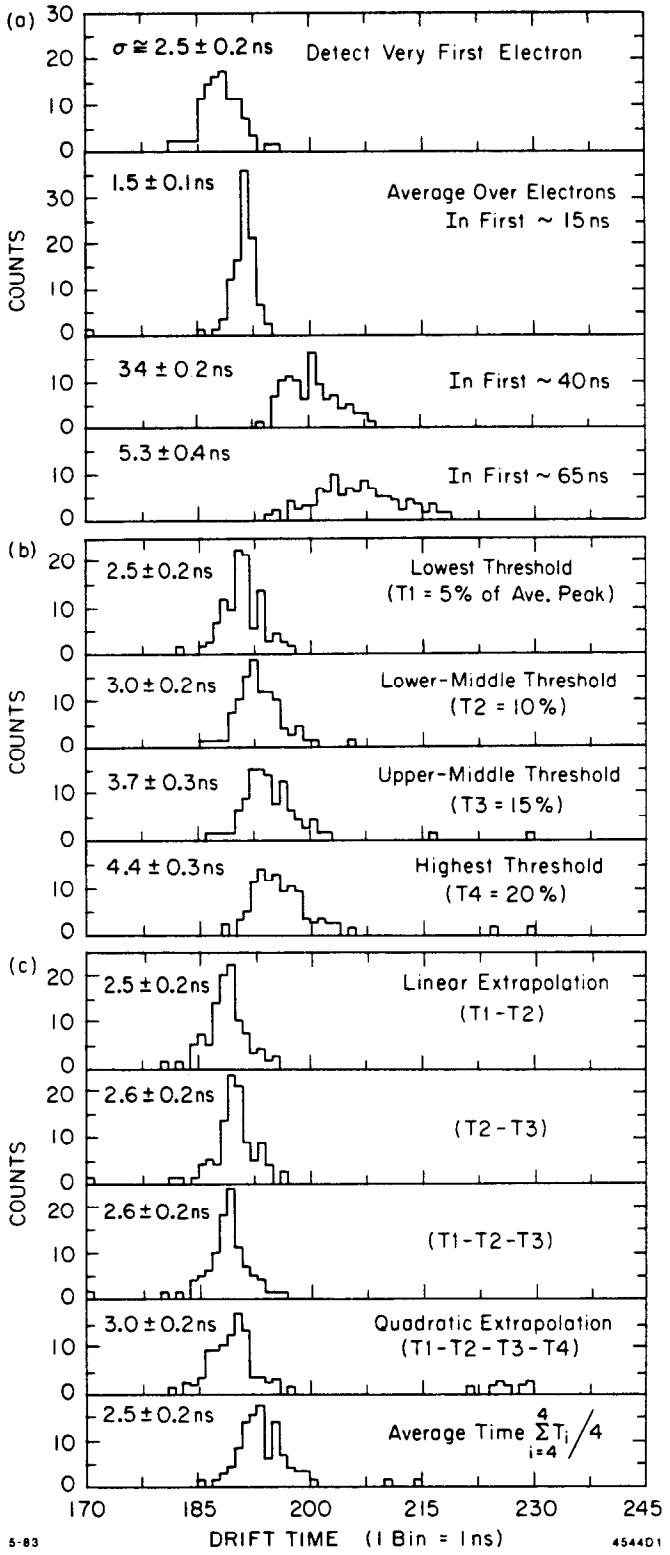

Fig. 4. Timing resolution obtained using drift pulses of Fig. 3, 90% Ar + 9% CO_2 + 1% CH_4, 10 kG, 1 atm, the impact parameter 7.5 mm and the drift velocity $v \simeq 45$ μm/ns. (a) A hypothetical timing using an infinitely fast electronics capable of digitizing every arriving electron; (b) timing with the drift pulses of Fig. 3 and the single threshold; and (c) with multiple thresholds.

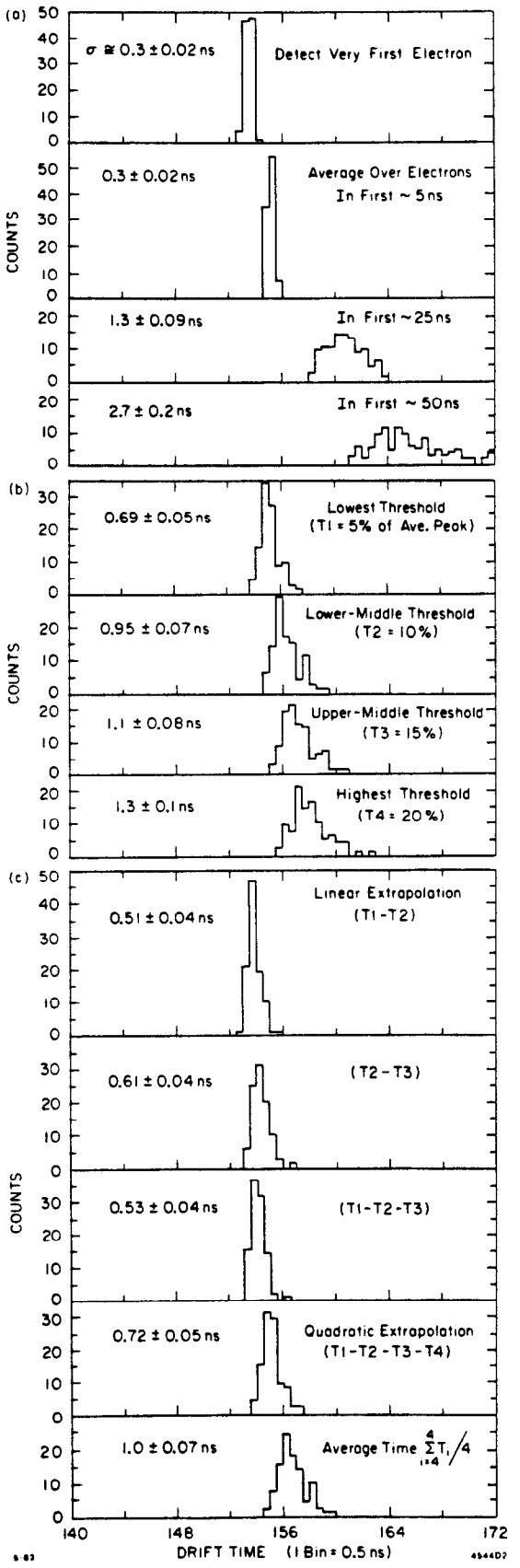

Fig. 5. The same conditions as in Fig. 4, except the pressure is 4 atm and $v \simeq 48$ μm/ns.

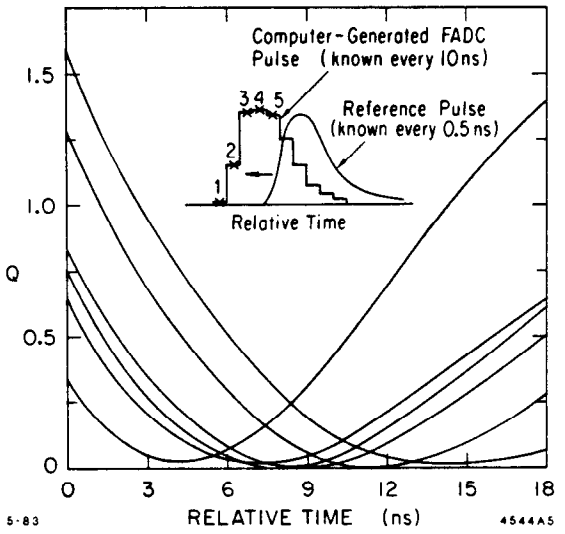

Fig. 6. The principle of the method of timing with the FADC using a reference pulse. The method minimizes a quantity $Q = \Sigma_{i=1}^{N} W_i[Y_i^{REF} - Y_i^{FADC}]^2$.

cells we would certainly prefer the weighted algorithm with 2-3 FADC points. Even then, our results with the leading edge algorithms are better, as one can see in Fig. 8.

The pressure is a very important variable to consider for FADC timing. As we go from 4 to 1 atm, the resolution gets worse by a factor 4-5. We have tried various things to improve the 1 atm results. For instance, we have speeded up the FADC clock to 5 ns and at the same time increased the rise time of the amplifier to 20 ns. We have observed only a marginal improvement. In fact that seems to be our conclusion; the FADC timing is rather insensitive to a method used. The reason for worse FADC timing in a small drift cell goes back to our discussion of the "U-shape" geometrical effect and the finite clustering ionization distributions. One should say, however, that as we increase the gain on the wire, one expects the improvement in the FADC timing simply because the later arriving ionization clusters will be suppressed by the saturation effects and the pulses will tend to be more smooth. In this limit the FADC timing will approach the leading edge timing.

EXAMPLE OF THE RESOLUTION IN A SMALL VERTEX JET CHAMBER

Much of the discussion from the previous chapter applies here too, of course. In this chapter we consider the design of the micro-jet chamber[5] where both the double track separation and the resolution are pushed to the best possible limit. In this particular discussion we consider 1 mm wire spacing. This dictates a small anode wire diameter (ϕ 7.8 μm chosen in the prototype) and this limits the overall length of such a chamber to 10-15 cm. This in turn means that the chamber could be assembled under the microscope to keep the mechanical tolerances within good limits. The chamber was coupled to a good low noise amplifier[8] with $\sim 2-3$ ns rise time to match a good rise time of the charge collection in this chamber.

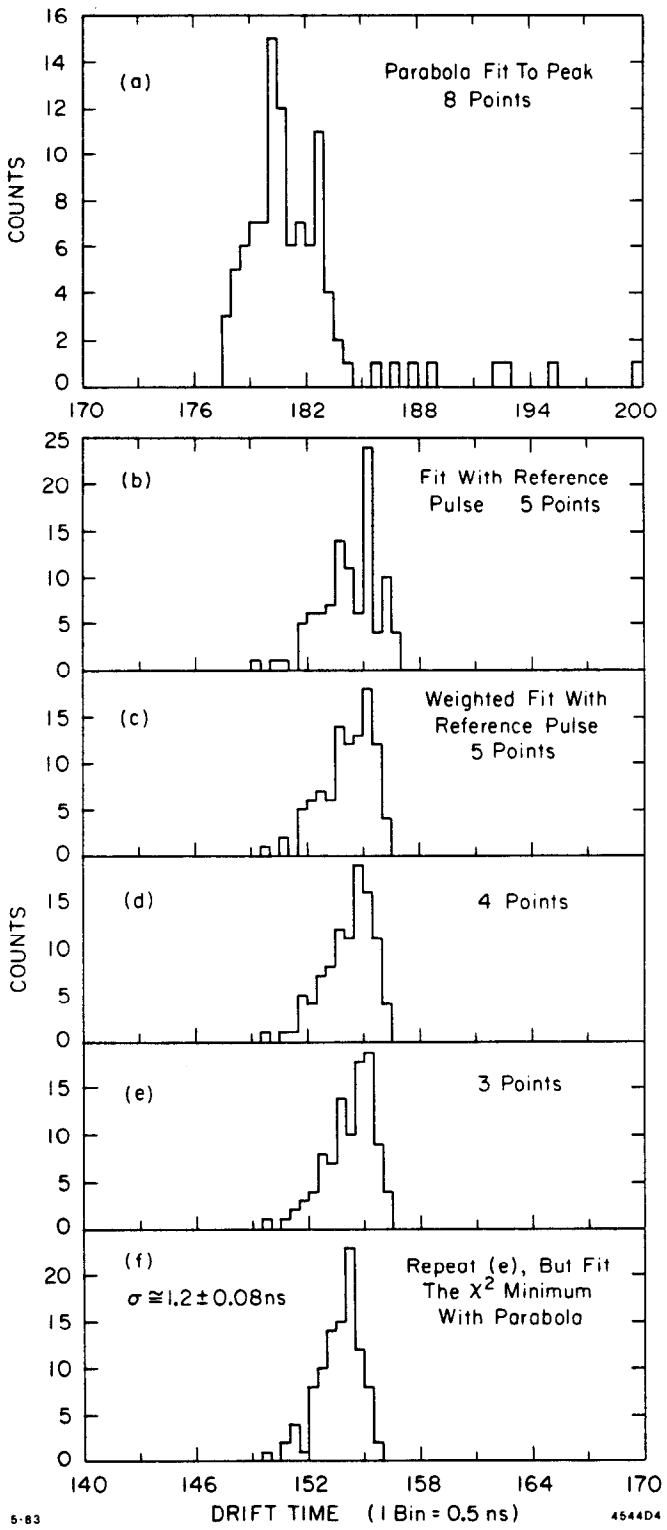

Fig. 7. The timing resolution obtained using the FADC simulation at 4 atm, 10 ns FADC clock and other conditions identical to Fig. 5. Case (a) is for a parabola fit using 8 FADC points with equal weight, (b) reference timing method of Fig. 6 with 5 FADC points of equal weight, (c)-(f) reference timing method with W1 = 4, W2 = 2, W3 = 1, W4 = 1, W5 = 1.

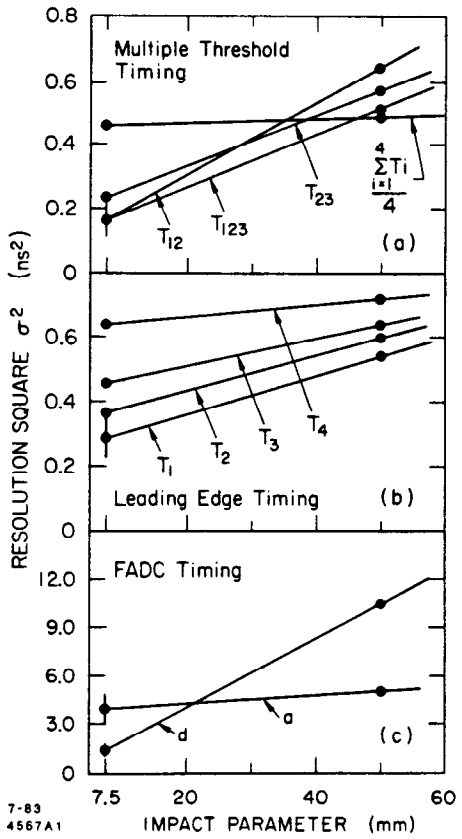

Fig. 8. Expected timing resolution as a function of the impact parameter for conditions identical to JADE cell,[6] 4 atm, 5 mm wire-wire spacing and v = 50.4 μm/ns. Cases (a) and (d) refer to Fig. 7.

Figure 9 shows the "U-shape" distributions in this structure (for a case of a full charge collection by the potential wires). One can see that only a small fraction of the sample length contributes to the first charge arrival. This has to be offset by higher pressure (4-6 atm) to achieve a good statistics. One should say that we do expect an improvement in the resolution if we bias the potential wires so that they do not collect the charge (the "U-shape" gets shallower). However, this improvement in resolution will be at the expense of the double track separation. A final requirement is to lower the diffusion by limiting the anode-cathode distance to only 4 mm. Figure 10 shows the computer generated drift pulses using a response of the above mentioned amplifier.[5],[9] The thresholds T1-T4 are set at 5, 10, 15 and 20% of the average peak value. Figure 11 shows the resolution study with (a) infinitely fast electronics, (b) with single threshold and (c) with multiple threshold technique using realistic drift pulses of Fig. 10. Again, as in the previous chapter, we see that the first electron timing is the best, and an ability to recover it if we use the double threshold method even at lower gain

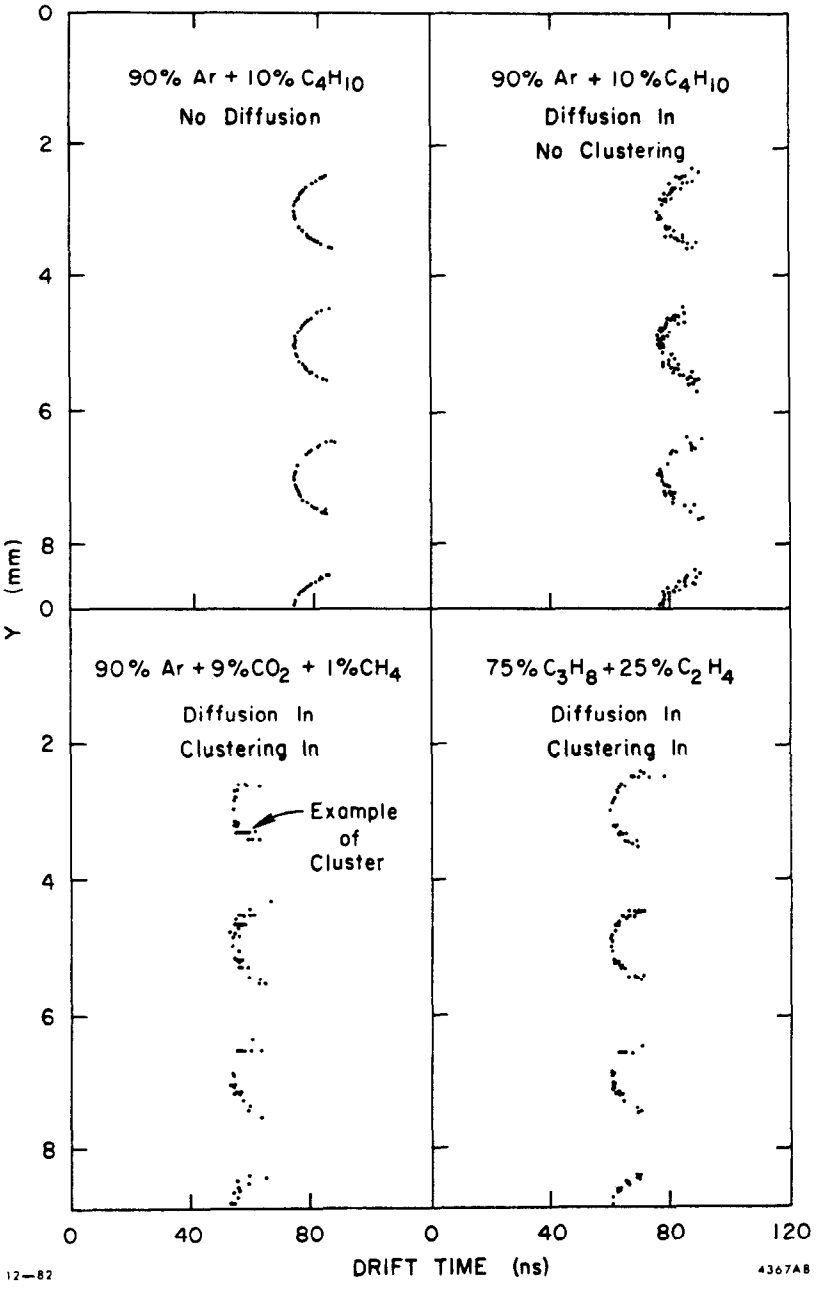

Fig. 9. The "U-shape" distributions in the micro-jet chamber[5] for a case when the potential wires fully collect the charge.

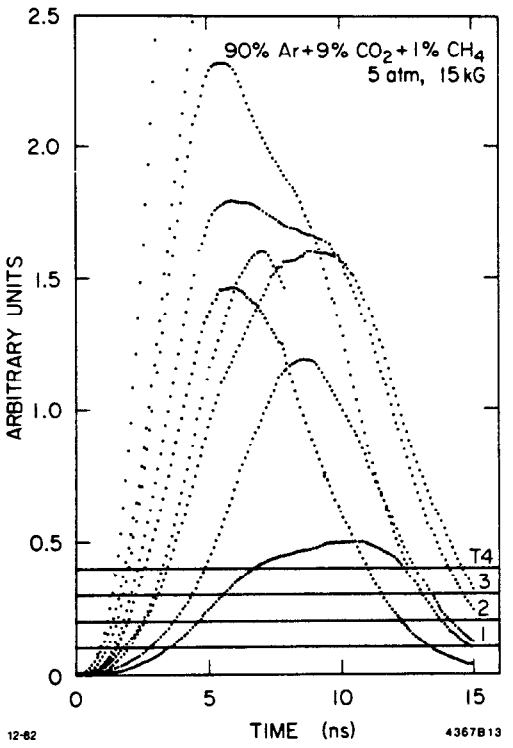

Fig. 10. The simulation of the drift pulses caused by particles in the micro-jet chamber.[5]

of the chamber. Figure 12 shows a comparison between the measurement and the program prediction assuming the first electron timing.[5]

The next question is whether we get some improvement in the resolution if we use some quality cut on the pulse shapes using an information based on the double threshold method. Figure 13 shows a correlation between the extrapolated time T_{23} and the time difference T3-T2 as we get it from the measurement using two thresholds. If we use this pulse height correlation to correct the time dispersion in T_{23} and at the same time apply a cut T3-T2 $\leq$ 0.4 ns, we can further improve the resolution – see Fig. 14. This resolution is somewhat better than the first electron timing – see Fig. 11, however, this is at the expense of a loss of $\sim$ 25% rejected events. Therefore, if one would consider this method, one should design the system with enough redundancy to allow a rejection of this fraction of samples. We would like to point out also, that this method is not equivalent to a constant fraction timing, because we have a capability to apply a quality cut on the pulse shapes.

CONCLUSIONS

The following are the conclusions of this study of the jet chamber geometry:

1. Although we have tried very hard to discover some trick in the timing method the conclusions are almost expected.

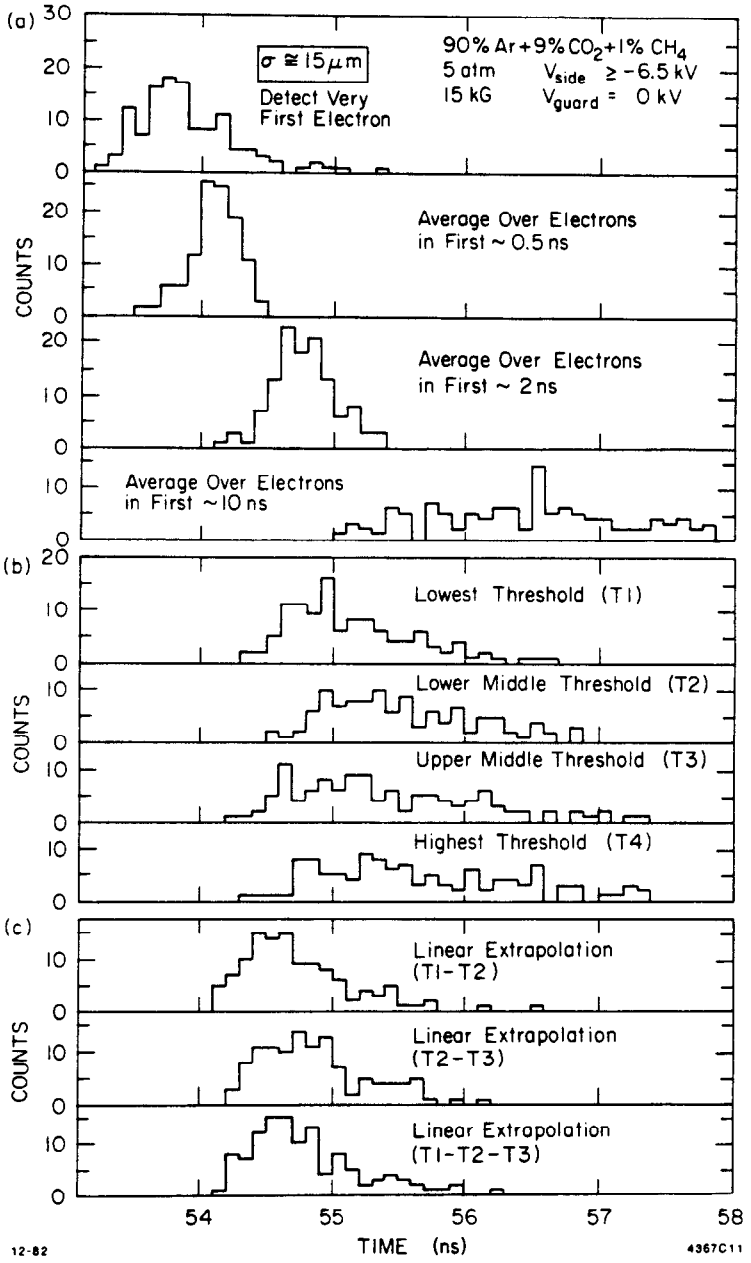

Fig. 11. The timing resolution in the micro-jet chamber[5] for 2 mm impact parameter, $v \simeq$ 45 μm/ns and using the pulse shapes of Fig. 10. Case (a) is for a hypothetical timing using an infinitely fast electronics, (b) single threshold timing and (c) multiple threshold timing using the realistic pulse shapes.

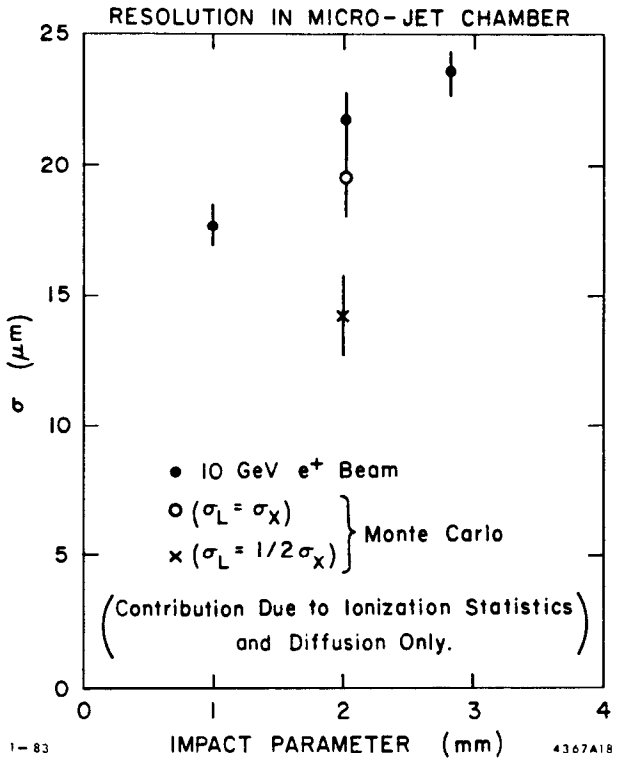

Fig. 12. Comparison of the experimental values[5] in 90% Ar + 10% C_4H_{10} gas, 6.1 atm and the program's simulation assuming a case of the first electron timing.

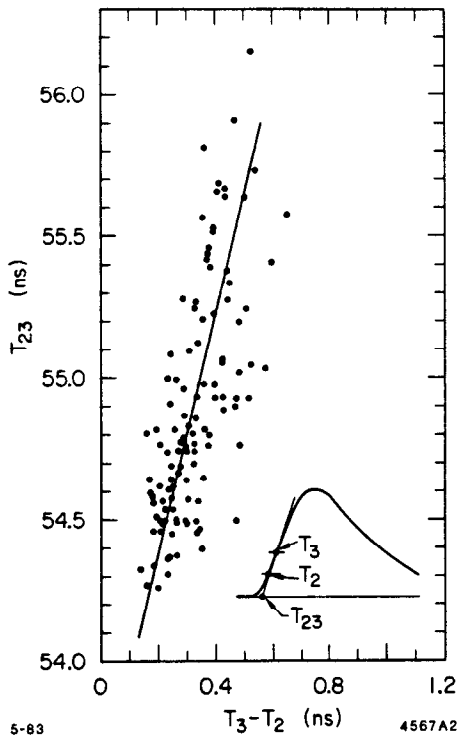

Fig. 13. The correlation of the projected timing point T_{23} and the time difference T3-T2 as obtained from the double threshold technique. The simulation corresponds to conditions of Fig. 11.

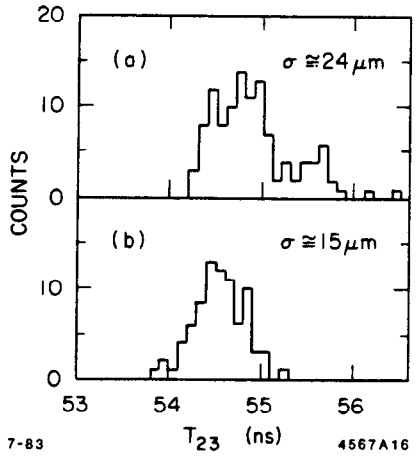

Fig. 14. (a) Double threshold timing resolution T_{23} accepting all events and without the use of the correlation of Fig. 13, (b) the corrected double threshold timing resolution T_{23} with the use of the correlation of Fig. 13 and in addition using the cut T3-T2 $\leq$ 0.4 ns. Both cases made for condition of Fig. 11.

2. The best accuracy one can obtain in the small vertex chambers is based on the first electron timing technique.
3. The double threshold technique should allow us to lower the gain in the chamber and still achieve the first electron timing quality. This result is yet to be checked experimentally.
4. The flash ADC timing with 10 ns clock makes sense in the chambers with the large drift length. However in the small vertex chambers it gives worse results compared to the leading edge timing unless one runs the chamber at a large gain (in that limit one expects similar results).
5. The improvement of the center of gravity timing over the first electron timing works in the limit of infinitely fast electronics and with the appropriate timing cuts. If we use the practical waveforms, the double threshold technique and apply the quality cut on pulse shapes, we can improve the first electron timing. However the price for this improvement is a loss of $\sim$ 25% samples, which has to be offset by a larger redundancy in the overall system. Again, this point has yet to be checked experimentally.
6. We believe that the further possible improvement in the resolution of the drift chambers might come from the electron focusing techniques ("time compression chambers"). However, to further improve on 10-20 μm resolution one would probably require some better choice of gases.

ACKNOWLEDGEMENTS

I would like to thank Dr. L. Keller for support during this project. I also would like to thank my summer student, L. Roberts, for software help which contributed to previously published work.[1],[2]

APPENDIX A

(Brief Description of the Drift Program)

There have been other attempts to simulate drift pulses;[11],[12] however, neither work was complete. We started from an electrostatic program,[13], which calculates a two-dimensional electrostatic field given the wire radii and potentials. The following are the main points of our analysis:

1. We create a segment of a track with clustering according to Piuz and Lapique.[3] Each electron within the cluster is drifted independently.
2. The drift velocity and diffusion is determined at each point according to the E/p and the magnetic field B.
3. The diffusion is simulated by randomizing each step, both in the longitudinal and transverse directions. The sigmas of the diffusions are taken from the measurement by parametrizing the longitudinal and transverse diffusion as a function of E/p. In the absence of such measurements we use

$$\sigma_x = \sigma_x^o \left(\frac{\epsilon_K x}{E}\right)^{1/2} \quad , \quad \sigma_L \sim \left\langle \frac{1}{2}\sigma_x , \sigma_x \right\rangle \quad ,$$

where x is the step length, $\epsilon_K = (E/p)^\alpha$ for $E/p >$ constant, $e_K = (\text{constant})^\alpha$ for $E/p <$ constant, E is the electric field, p is the pressure and σ_x^o is the normalization constant. (We use $\sigma_x^o = 380$ μm normalized at 1 kV/cm, 1 atm and 1 cm of drift; $\alpha = 1.3$ and constant $= 0.02$ kV/cm for 90% Ar + 10% C_4H_{10}).

4. The avalanche fluctuation is simulated by assigning a weight x to each electron according to the following weighting function, A(x) = constant $xe^{-1.5x}$.[15]
5. The effect of the positive ions is simulated by convoluting the drift time distribution with a function

$$i(t) \propto \frac{1}{1 + t/p \cdot t_0} \quad ,$$

where $t_0 = r_a/2\mu E_a \sim 0.1 - 0.2$ ns for $r_a = 3.9$ μm, $\mu \sim 1.5$ cm^2 V^{-1} sec^{-1}, $E_a \simeq$ 940 kV/cm in the micro-jet chamber and 90% Ar + 10% C_4H_{10} gas.

6. The effect of the electronics is simulated semi-empirically by measuring an amplifier's response to an impulse charge and convoluting this function with the rest of the distribution. At this point we include the effect of filters and noise.

REFERENCES

1. J. Va'vra, L. Roberts, D. Freytag and P. Clancey, Nucl. Instrum. Methods 203 (1982) 109-118.
2. J. Va'vra and L. Roberts, SLC Workshop Note #31, 1982.
3. J. Va'vra, Internal Notes for the New Detector Group at SLAC, 1982, and SLD Proposal for the SLC Experiment, 1982.
4. G. Tarnopolsky, 1983 Wirechamber Conference, Vienna, Austria.
5. J. Va'vra, SLAC-PUB-3045 and SLAC-PUB-3130, and 1983 Wirechamber Conference, Vienna, Austria.
6. H. Drumm et al., Nucl. Instrum. Methods 176 (1980) 333-344.
7. D. Cockerill et al., Nucl. Instrum. Methods 176 (1980) 159-162.
8. OPAL Technical Proposal, CERN/LEPC/83-4.
9. R. A. Boie, A. T. Hrisoho and P. Rehak, Nucl. Instrum. Methods 192 (1982) 365-374.
10. A. H. Walenta et al., 1983 Wirechamber Conference, Vienna, Austria.
11. G. R. Ricker and J. J. Gomes, The Rev. of Sci. Instrum. 40 (1969) 227.
12. K. Bunnell, MARK III Program (1979), unpublished.
13. D. Miller and R. H. Schinder, MARK II Program (1978), unpublished.
14. F. Lapique and F. Piuz, Nucl. Instrum. Methods 175 (1980) 297.
15. S. C. Curran, A. L. Cocroft and J. Angus, Philos. Mag. 40 (1949) 929.

SLAC-PUB-3131 Errata
September 1983
(I)

SEARCH FOR THE BEST TIMING STRATEGY IN HIGH PRECISION DRIFT CHAMBERS*

J. VA'VRA
Stanford Linear Accelerator Center
Stanford University, Stanford, California 94305

p. 1 3rd line, distribution category: for "(T/E)" read "(I)"

p. 4 2nd line, figure caption: for ".5 mm" read "7.5 mm"

p. 9 2nd line from bottom, for "amplifier[8]" read "amplifier[9]"

---

* Work supported by the Department of Energy, contract DE-AC03-76SF00515.